American Mineralogist, Volume 76, pages 904–912, 1991

Scanning calorimetric measurement of heat capacity during incongruent melting of diopside

REBECCA A. LANGE, JAMES J. DE YOREO,* ALEXANDRA NAVROTSKY
Department of Geological and Geophysical Sciences, Princeton University, Princeton, New Jersey 08544, U.S.A.

ABSTRACT

Scanning calorimetric measurements (in step-scan mode) using a Setaram HT1500 calorimeter were performed on initially crystalline diopside ($CaMgSi_2O_6$) between 1403 and 1762 K and provide a direct measurement of heat capacity. Incongruent melting begins approximately 59 K below the melting point reported previously of 1665 K. Backscattered electron imaging confirms that the starting crystalline sample is a single phase at a resolution of ≥ 1 μm. The diopside is stoichiometric to $\pm 2\%$ (resolution of electron microprobe analysis). The observed incongruency, which has been noted previously, is therefore intrinsic to pure $CaMgSi_2O_6$ and not related to the presence of other phases or to deviations in the Ca/Mg ratio from unity. The first 20% of melting occurs over an interval of 44 K and the remaining 80% within 15 K. Measurements of heat capacity of crystalline and liquid diopside (outside the melting interval) scatter within 5 and 12%, respectively, of the accepted literature values. The integrated heat contents, in both the crystalline and liquid regions, are within 0.3% of reported values. The enthalpy of fusion is 137.7 kJ/mol, in excellent agreement with previous determinations (Stebbins et al., 1983; Richet and Bottinga, 1984; Ziegler and Navrotsky, 1986). Continuous scanning measurements during cooling of diopside liquid at different rates produce a large heat effect at temperatures well below the melting point reported previously. This heat effect can be correlated with the simultaneous crystallization of a clinopyroxene solid solution and wollastonite. Scanning measurements at a constant cooling rate of 10 K/h were repeated three times under identical conditions; each time the observed heat effect, indicating crystallization, took place at a different temperature (1576, 1534, and 1566 K). These observations are in general agreement with the kinetic crystallization study of Kirkpatrick et al. (1981), although metastable crystallization of forsterite was not detected in our cooling experiments.

INTRODUCTION

The transformation between the liquid and solid states is central to igneous processes, both in the generation of melts from a mineral assemblage and in their subsequent ascent and crystallization. Mineral heats of fusion thus play a critical role in governing the evolution of the crust and mantle. In recent years, accurate data on the enthalpy of fusion have been obtained for various minerals with high melting points (Stebbins et al., 1983; Richet and Bottinga, 1984; Ziegler and Navrotsky, 1986). Such data are becoming increasingly important as thermodynamic models of crystal-melt equilibria grow in sophistication and success (Berman and Brown, 1984, 1987; Ghiorso et al., 1983; Ghiorso and Carmichael, 1985; Ghiorso, 1987). Accurate heats of fusion are particularly important for the definition of standard states for the components of more complex silicate liquid and solid solutions. Moreover, mineral heats of fusion provide the largest contribution to the evolving heat content of a magma as it cools and crystallizes, such that models of a magma's thermal evolution (Brandeis and Jaupart, 1984; Ghiorso, 1991) depend critically on accurate data on the enthalpy of fusion, and on the distribution of this enthalpy over a large liquidus interval.

Most determinations of the heats of fusion of minerals with high melting points have been obtained by traditional drop calorimetry, where a sample dropped from high temperature into a calorimeter at room temperature yields H_T-H_{298}. Stebbins et al. (1983), Richet and Bottinga (1984), and Ziegler and Navrotsky (1986) reviewed the problems inherent in this approach when applied to materials that quench to form a glass or a mixture of glass and crystals, and they outlined the corrections required to interpret the results. Direct measurements of enthalpy of fusion can be made by transposed-temperature drop calorimetry (Gaune-Escard and Bros, 19874; Castanet and Bergman, 1977; Pool et al., 1979; Ziegler and Navrotsky, 1986). This method involves dropping a well-characterized crystalline sample equilibrated at room temperature into a hot calorimeter. Fusion thus takes place in the calorimeter, and problems of glass formation are completely avoided. Recently, Ziegler and Navrotsky (1986) reported the direct measurement of the enthalpy of fusion

* Present address: Lawrence Livermore Laboratory, Livermore, California 94550, U.S.A.

0003–004X/91/0506–0904$02.00

of diopside using the transposed-temperature drop technique with a Setaram HT1500 calorimeter. Their measurement of the enthalpy of fusion, 138.5 kJ/mol, at 1665 K, the previously reported melting point of diopside and their derived value for the average heat capacity of diopside liquid, 334 J/mol·K, are both in excellent agreement with previous studies on diopside based on conventional drop methods (Ferrier, 1968; Stebbins et al., 1983; Richet and Bottinga, 1984). The measurements of Ziegler and Navrotsky (1986) confirmed the incongruent melting of diopside initially reported by Biggar and O'Hara (1969) and Kushiro (1973). Ziegler and Navrotsky (1986) observed a rise in the enthalpy of diopside approximately 31 K below its previously reported melting point. The incongruent behavior could not be detected by either Stebbins et al. (1983) or Richet and Bottinga (1984), since diopside liquid quenched to a glass in their drop experiments.

We note that incongruent melting of diopside will always be observed if the starting material has been crystallized directly from the liquid state. This is due to the sluggish nucleation of diopside over a wide range of cooling rates, which has been documented in the crystallization experiments of Kirkpatrick et al. (1981). As a consequence, crystallization from stoichiometric diopside melt typically results in a three-phase assemblage, forsterite + wollastonite + clinopyroxene solid solution, with the exact phase proportions and compositions dependent on the cooling rate. Thus, any report of incongruent melting of pure crystalline diopside must first verify that the starting material consisted of a stoichiometric single phase.

This paper reports a scanning calorimetric study on crystalline diopside through its melting interval. Scanning calorimetry consists of measuring the change in heat of a sample during heating (or cooling) at a constant rate and thus provides a direct measurement of heat capacity. This approach is particularly useful when applied to compounds that melt incongruently, since measurements of the derivative property, heat capacity, provide a more sensitive probe of melting than measurements of the integral property, enthalpy, obtained by drop methods. The scanning method can also be applied to kinetic studies of crystallization, as the heat effect resulting from crystallization can be monitored while the sample is cooled at a constant rate. The purposes of this study are (1) to verify the incongruent melting of diopside and determine the temperature at which melting begins, (2) to simulate the crystallization experiments of Kirkpatrick et al. (1981) at different cooling rates in an attempt to identify and quantify the heat effect resulting from the crystallization of forsterite prior to that of wollastonite and a clinopyroxene solid solution, and (3) to evaluate the precision and accuracy of heat capacity data obtained by the scanning method at high temperatures.

Experimental methods

The initial starting material was diopside glass prepared by Lange and Carmichael (1987). The composition of the glass was determined by electron microprobe analysis (Table 1) using the JEOL 8600 electron microprobe at Rutgers University. Chunks of the diopside glass (1–2 g) were crystallized at 1523 K for 48 h. Electron microprobe analyses of the crystal and glass are provided in Table 1. Both conform closely to stoichiometric (ideal) diopside, and the measured glass composition is consistent with the wet chemical analysis reported by Lange and Carmichael (1987). The crystalline diopside was found to be single phase by optical microscopy. Individual grains were examined using backscattered electron imaging; only one phase was present at a resolution of ≥ 1 μm. Powder X-ray diffraction (XRD) analyses were also performed on the crystalline diopside sample, and the lack of peaks from forsterite and wollastonite indicates that neither phase is present within the detection limit of the XRD ($\sim$2%).

Table 1. Composition of glassy and crystalline diopside (wt%)

	Crystal*	Glass*	Glass**	Ideal
SiO_2	55.75(0.64)	55.50(0.58)	55.72	55.49
MgO	18.15(0.32)	18.25(0.30)	18.43	18.61
CaO	25.78(0.51)	26.11(0.41)	25.75	25.90
Total	99.67	99.86	99.90	100.00
Si	2.01	2.00	2.01	2.00
Mg	0.98	0.98	0.99	1.00
Ca	0.99	1.01	0.99	1.00
O	6.00	6.00	6.00	6.00

* Electron microprobe analysis (standard deviations in parentheses).
** Wet chemical analysis of Lange and Carmichael (1987; standard deviation = ±1%).

Calorimetric measurements were made in a Setaram HT1500 calorimeter (Gaune-Escard and Bros, 1974; Ziegler and Navrotsky, 1986). The calorimetric detector (Fig. 1) consists of an upper thermopile surrounding an alumina sample crucible with a Pt inner crucible, and a lower thermopile surrounding an alumina reference crucible. The measurements of this study were obtained by operating the calorimeter in step-scanning mode. The sample was loaded into the calorimetric detector before the furnace was heated. The reference crucible was half filled with dried corundum powder, whereas the sample crucible held a snugly fitting Pt crucible with a Pt-foil lid that was empty (a blank), filled with tamped corundum powder (a standard), or filled with tamped crystalline diopside powder (a sample). Separate Pt crucibles (weighing $\sim$2 g and within 0.05 g of each other) were used to prevent problems of contamination and to allow rapid changes between standard and sample without waiting for the crucibles to be cleaned. The corundum powder (0.94967 g) was dried at 1773 K before being tamped into the Pt crucible, whereas the diopside powder (1.30602 g) was dried at 1523 K.

Each scanning experiment consisted of three parts: a blank, a calibration, and a sample. One experiment involved monitoring the calorimetric signal as the temperature was raised (or lowered) quickly over a temperature interval of 5 K (see Fig. 2). The voltage changed rapidly

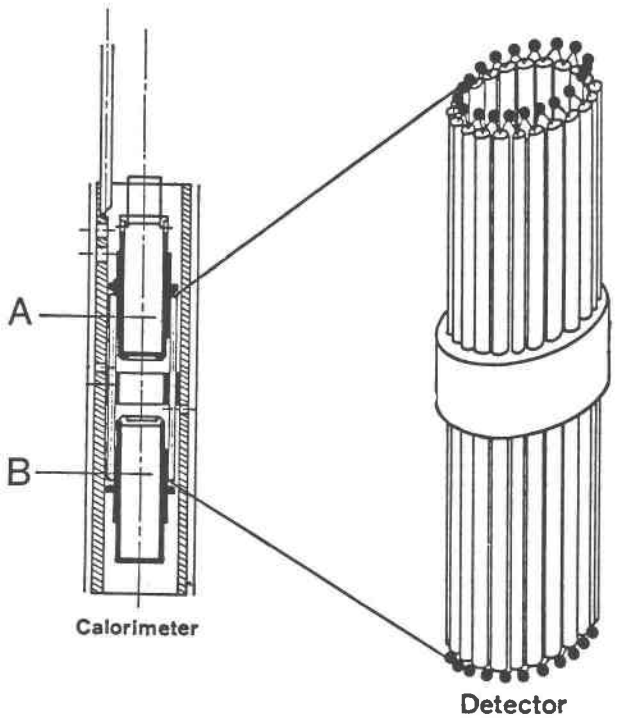

Fig. 1. Detail of the calorimetric detector. The picture on the left shows the sample (A) and reference (B) crucibles in position in the calorimeter. The diopside powder was tamped into a Pt crucible that was fitted snugly within the upper alumina crucible (A). The lower alumina crucible (B) serves as a reference and was partially filled with dried corundum powder. The picture on the right shows the detail of the thermopiles that surround the crucibles. The calorimeter as shown was suspended and centered in a 10-cm isothermal zone of a graphite furnace.

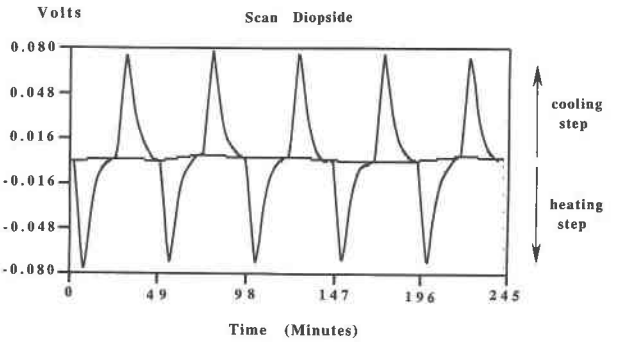

Fig. 2. Typical plot of voltage vs. time during ten alternating heating and cooling scanning steps. In this example, the diopside sample (equilibrated at 1624 K for 90 min) was initially heated at a rate of 1 K/min for 5 min followed by an isothermal interval of 20 min. The sample was then cooled at a rate of 1 K/min for 5 min followed by another isothermal period. Note that the baseline remained flat throughout all ten steps, indicating that the calorimetric detector was well balanced in terms of the heat capacities of the reference and sample chambers. The area under each peak was calculated, and the average of these ten values was taken as one datum.

during a heating (or cooling) step because of the difference in heat capacity between the materials in the upper and lower chambers of the detector. After a heating period, an isothermal interval followed until the signal returned to base line. Although the sample temperature came to within 0.5 K of the final temperature within 1–2 min after heating, the calorimetric detector typically took about 20 min to equilibrate. It is this temperature lag of the detector behind that of the sample which is the principal reason for performing the scanning experiments in step mode rather than continuously.

The area under the voltage peak after each step-scan cycle (Fig. 2) is proportional to the integral of the average heat capacity of the material in the sample chamber over the temperature interval scanned. If the temperature interval is small, then changes in the heat capacity will also be small, and the average heat capacity can be assigned to the midpoint temperature. A typical experiment outside the melting interval (Fig. 2) consisted of ten alternating heating and cooling steps, each at a rate of 1 K/min for 5 min followed by a 20-min isothermal period. The average of these ten values was taken as one datum point. The results of the scans of the blank were subtracted from those of the standard and sample, and corrections were applied for the small differences in weight among the three Pt crucibles. The scans with corundum provided a calibration factor.

Experiments performed within the melting interval differed from those described above in that they consisted of ten continuous heating steps at a rate of 1 K/min for 5 min followed by a 20-min isothermal period. The area under each peak led to calculated values of C_P that are identical within error to those conducted in alternating heating and cooling steps during the first 40 K of the melting interval (1605–1645 K). It is only during the last 20 K of melting (1645–1665 K) that alternating heating and cooling steps cannot be conducted successfully. This is because the proportion of crystals + liquid changes significantly over this latter part of the melting interval. As a result, melting rates on heating are more rapid than crystallization rates on cooling, reflecting the sluggish kinetics of crystallization. We do note, however, that heating steps of 1 K/min for different durations of 2, 5, and 10 min all led to identical measurements of the heat capacity function over the melting interval; this indicates that melting rates are close to equilibrium during these heating steps.

The temperature gradient in the furnace was measured at several temperatures, and the isothermal zone was found to be approximately 10 cm long. The calorimetric detector was centered in the graphite furnace tube so that the temperature varied by less than 2 K over the entire detector assembly at all temperatures. The temperature in the calorimeter was read with a thermocouple (Pt-6%Rh/Pt-30%Rh) located next to the sample crucible. The calibration of this thermocouple was checked by

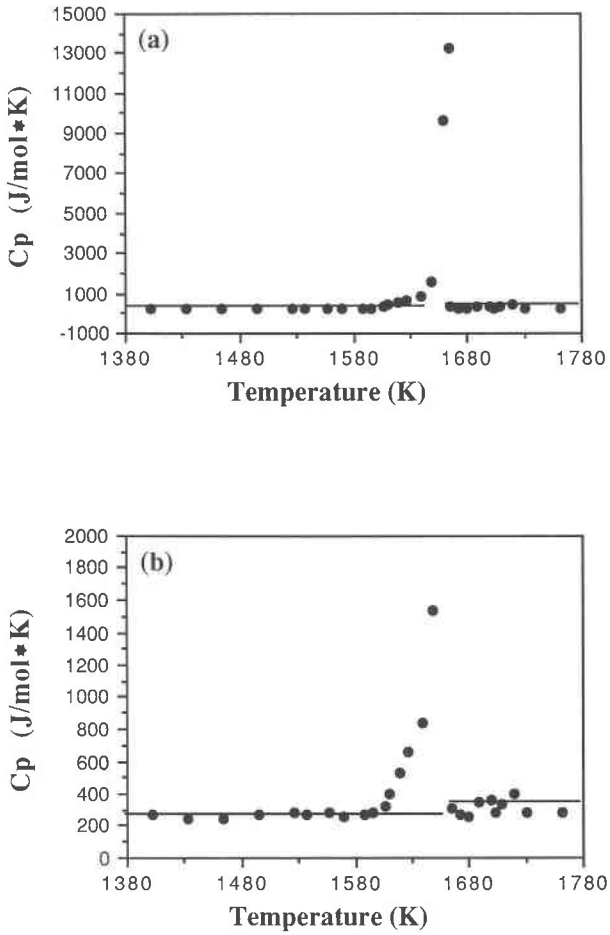

Fig. 3. Plots of measured heat capacity vs. temperature during incongruent melting of diopside. Two scales are presented: (a) a C_P scale up to 15000 J/mol·K to illustrate all measured points and (b) a C_P scale reduced to 2000 J/mol·K to provide better detail of the melting behavior of diopside. Straight lines are fitted heat capacity equations of Stebbins et al. (1983; crystalline region) and Richet and Bottinga (1984; liquid region).

melting a Au sample (1337 K) in the alumina sample chamber.

Data acquisition and analysis were accomplished with an IBM-compatible PC with a National Instruments IEE-488 interface (GPIB) board communicating with a Keithley 181 nanovoltmeter. The software was written by the second author (J.D.).

Heat capacity of crystal and liquid, enthalpy of fusion, and analysis of error

Data were collected between 1403 and 1762 K and reduced using the following relationship:

$$C_P(T)_{\text{diopside}} = [(A/\Delta T)_{\text{diopside}} - (A/\Delta T)_{\text{blank}})]\ (\gamma M_s/m_s) \quad (1)$$

where $T = (T_2 + T_1)/2$ and T_2 and T_1 bracket the scanning temperature interval (5 K), $\Delta T = T_2 - T_1$, M_s = molecular weight of diopside, m_s = mass of diopside, and

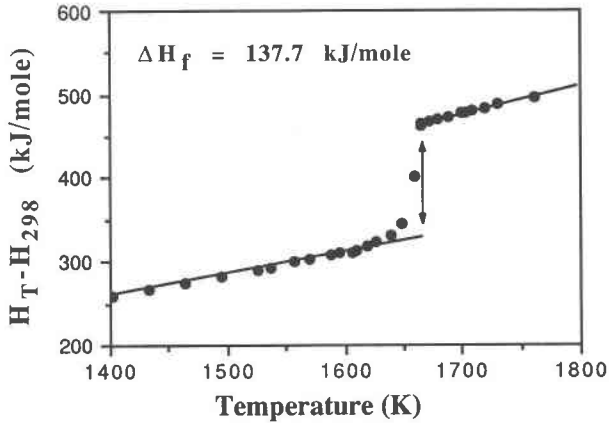

Fig. 4. Enthalpy (referenced to crystalline diopside) vs. temperature calculated from the scanning measurements of heat capacity. The fitted equation of Stebbins et al. (1983) is used to calculate H_{1403}-H_{298}. The incongruent melting of diopside is not evident from this diagram until ~1630 K (~25 K higher than seen with the C_P data). The enthalpy fusion is 137.7 kJ/mol (see text).

A = integrated area under voltage peak (average of ten peaks) and

$$\gamma \text{ (calibration factor)} = [(m_{Al_2O_3} C_P(T)_{Al_2O_3}/M_{Al_2O_3}] / [(A/\Delta T)_{Al_2O_3} - (A/\Delta T)_{\text{blank}}] \quad (2)$$

where $C_P(T)_{Al_2O_3}$ = heat capacity of corundum from Robie et al. (1979), $m_{Al_2O_3}$ = mass of corundum, and $M_{Al_2O_3}$ = molecular weight of corundum. The calibration factors increased as the temperature of the experiments increased, indicating a decrease in sensitivity with increasing temperature. As suggested by Ziegler and Navrotsky (1986), this is probably the result of an increase in the transfer of heat by radiation relative to the heat transferred through the thermopile at high temperatures.

The heat capacities between 1403 and 1762 K are reported in Table 2 and Figures 3a and 3b. The most striking feature is the abrupt rise in heat capacity at approximately 1606 K. The heat capacity reaches a maximum near 1665 K, the previously reported melting point of diopside, and then abruptly falls after melting is complete. These data indicate an incongruent melting interval for diopside of about 59 K, a much wider range than that resolved from the enthalpy data of Ziegler and Navrotsky (1986), 31 K. This discrepancy, however, merely reflects the difference in resolution obtained between measurements of derivative and integral properties. In fact, the onset of melting cannot be seen from our integrated data of heat content (Fig. 4) until approximately 1630 K, only 35 K below the melting point reported previously.

Heat contents were calculated by integrating the scanning measurements of heat capacity using the following relationship:

$$H_T - H_{T^0} = \int_{T^0}^{T} C_P(T)\, dT \quad (3)$$

TABLE 2. Diopside heat capacity and enthalpy data

Phase	T K	C_P J/mol·K (meas)	C_P J/mol·K (calc[1])	Δ %	H_T-H_{298} kJ/mol (meas)	H_T-H_{298} kJ/mol (calc[2])	Δ %
c	1403	265.34	259.54	2.23	258.93	258.93	0.00
c	1433	245.88	259.85	−5.38	266.60	266.70	−0.04
c	1464	246.77	260.14	−5.14	274.23	274.74	−0.18
c	1496	267.27	260.43	2.63	283.46	283.06	−0.14
c	1527	283.92	260.69	8.91	291.00	291.12	−0.04
c	1537	271.23	260.77	4.05	293.78	293.72	0.02
c	1558	280.05	260.94	7.32	299.56	299.19	0.12
c	1570	253.31	261.03	−2.96	302.76	302.32	0.15
c	1589	276.80	261.17	5.98	307.80	307.27	0.17
c	1596	279.99	261.22	7.19	309.75	309.10	0.21
c-l	1606	324.61	261.25	24.25	310.67	309.71	0.31
c-l	1610	397.88	261.33	52.25	314.70	312.75	0.62
c-l	1620	522.80	261.40	100.0	319.30	315.36	1.25
c-l	1627	658.11	261.44	151.73	323.44	317.19	1.97
c-l	1639	839.13	261.53	220.85	332.42	320.33	3.77
c-l	1649	1535.56	261.60	486.99	344.89	323.08	6.75
c-l	1659	9622.81	261.66	3577.60	400.68	325.69	23.02
c-l	1663	13261.71	261.70	4967.52	463.61	327.13	41.72
l	1673	273.34	334.00	−18.16	469.20	467.63	0.34
l	1679	263.97	334.00	−20.97	470.95	469.81	0.24
l	1689	342.47	334.00	2.53	473.98	473.15	0.17
l	1699	363.23	334.00	8.75	477.51	476.49	0.21
l	1703	281.94	334.00	−15.59	478.64	477.66	0.21
l	1709	341.72	334.00	2.31	480.66	479.83	0.17
l	1719	395.29	334.00	18.35	484.35	483.17	0.24
l	1731	283.25	334.00	−15.15	488.42	487.21	0.25
l	1762	283.40	334.00	−15.15	497.21	497.53	−0.06
scl	1641	306.80	334.00	−8.14	459.45	458.87	0.13
scl	1610	321.03	334.00	−3.88	449.72	448.51	0.27

Note: Abbreviations: meas = measured in this study; calc[1] = calculated from Equation 5 in text; calc[2] = calculated from Equation 4 in text; Δ = [(meas − calc)/calc]100; c = crystal; l = liquid; c-l = crystal + liquid; scl = supercooled liquid.

where T^0 is the lowest temperature (1403 K) at which a heat capacity measurement was obtained. Area integration was performed by cubic interpolation of the data points with the stipulation that at 1665 K the heat capacity reach a maximum. To reference the integrated heat contents to 298 K and to facilitate comparison with other studies, the equation of Stebbins et al. (1983),

$$H_T\text{-}H_{298} = 0.2439\ T + 5.3451 \times 10^{-6}\ T^2 - 93.6894\ \text{kJ/mol} \quad (4)$$

for crystalline diopside was used to calculate H_{1403}-H_{298}. This quantity, 258.93 kJ/mol, (Table 2, first entry) is the starting point relative to which heat contents for diopside are calculated using the scanning measurements of heat capacity. These heat content data are compared in Table 2 and Figure 4, at temperatures below the onset of melting, to values of H_T-H_{298} calculated directly from the equation of Stebbins et al. (1983). This equation is based on the drop calorimetry data of White (1919), Wagner (1932), and Ferrier (1968), which have a standard deviation in enthalpy of ±2.3 kJ/mol. Thus, the agreement of our integrated heat content data within 0.3% of those calculated from Equation 4 is well within the error of the drop measurements on crystalline diopside.

Stebbins et al. (1983) also presented an equation for the heat capacity of crystalline diopside,

$$C_P(T) = 264.8 + 9.46 \times 10^{-4}\ T - 12.958 \times 10^6\ T^{-2}\ \text{J/mol·K} \quad (5)$$

calibrated on the same enthalpy data as the fit in Equation 4. A comparison between the heat capacities calculated from this equation and those obtained from the scanning measurements is provided in Table 2. The equation presented by Berman and Brown (1985) for the heat capacity of crystalline diopside leads to values that are within 0.7% of those calculated from Equation 5 between 1400 and 1665 K. The measurements from this study scatter about other values reported by 5% on average. This is slightly larger than the estimated propagated error in heat capacity of 3.5% when derived from the drop measurements of enthalpy. The marked deviation in our measurements of heat capacity beginning at 1606 K cannot be directly compared to values generated from Equation 5 because the data upon which the equation is fitted were obtained at temperatures ≤1573 K. Although Ferrier (1968) presented enthalpy data for crystalline diopside between 1573 and 1665 K on a graph, the actual data were not tabulated; it is thus difficult to assess whether incongruent melting was observed. Nor can our measurements of incongruent melting of crystalline diopside be compared to the more recent studies of Stebbins et al. (1983) and Richet and Bottinga (1984) because the starting materials in both studies were diopside glass and not crystalline diopside.

The scanning calorimetric measurements of heat capacity were extended into the liquid region (Table 2) and allow integrated heat contents to be calculated up to 1762 K. These data are compared directly in Figure 5 with the

liquid enthalpy measurements of Stebbins et al. (1983) and Richet and Bottinga (1984), corrected to the crystalline reference state. The agreement among all three studies is remarkably good, especially given the scatter in the scanning calorimetric measurements of liquid heat capacity. If the heat capacity of liquid diopside is assumed to be constant, then the mean value from our scanning measurements is 312 J/mol·K with a standard deviation and a standard error of ±40 and ±10 J/mol·K, respectively. Regression of our integrated enthalpy data, assuming a linear dependence on temperature,

$$H_{T\text{liq}}\text{-}H_{298\text{crystal}} = a + bT \quad (6)$$

leads to a value for b, equivalent to the heat capacity of liquid diopside, 312 ± 10 J/mol·K. Both our average and fitted values for the heat capacity of liquid diopside are about 20 J/mol·K lower than the value of 334 J/mol·K reported both by Richet and Bottinga (1984) and Ziegler and Navrotsky (1986). In turn, this latter value is about 20 J/mol lower than that reported by Stebbins et al. (1984), 353 J/mol·K. When the integrated liquid enthalpies calculated in this study are combined with the liquid enthalpies of Stebbins et al. (1983) and Richet and Bottinga (1984), an average liquid heat capacity for diopside of 334 J/mol·K is obtained. Although the fitted error on this value is ±7 J/mol·K, a more accurate estimate of the uncertainty, based upon the combined uncertainties in the liquid enthalpy data from all three studies, is about ±20 J/mol·K.

The primary focus of the studies of both Stebbins et al. (1983) and Richet and Bottinga (1984) was the measurement of an enthalpy of fusion. Their reported values, 138.1 and 137.7 kJ/mol, respectively, are in close agreement and are derived by assuming a single fusion temperature at 1665 K. Stebbins et al. (1983) and Richet and Bottinga (1984) employed the enthalpy data for crystalline diopside of White (1919), Wagner (1932), and Ferrier (1968) extrapolated up to 1665 K and their own measurements of enthalpy in the liquid region (referenced to the crystalline state) to calculate

$$\Delta H_{f,1665} = (H_{1665\text{liq}}\text{-}H_{298\text{crystal}}) - (H_{1665\text{crystal}}\text{-}H_{298\text{crystal}}). \quad (7)$$

The error in $\Delta H_{f,1665}$ is about ±3 kJ/mol and stems from the standard deviation in the data for crystalline diopside and the uncertainty introduced to the liquid data during correction to a crystalline reference state.

Our derived enthalpy of fusion is obtained from the total change in enthalpy over the melting interval. This total enthalpy change is calculated by integrating the observed heat capacity data between 1606 and 1665 K. It can also be expressed as the integrated heat capacity of crystalline diopside extrapolated to 1665 K plus a heat of fusion term at 1665 K:

$$\Delta H_{\text{total}} = \int_{1606}^{1665} C_P(T)_{\text{obs}}\, dT = \int_{1606}^{1665} C_P(T)_{\text{xtl}}\, dT + \Delta H_{f,1665}. \quad (8)$$

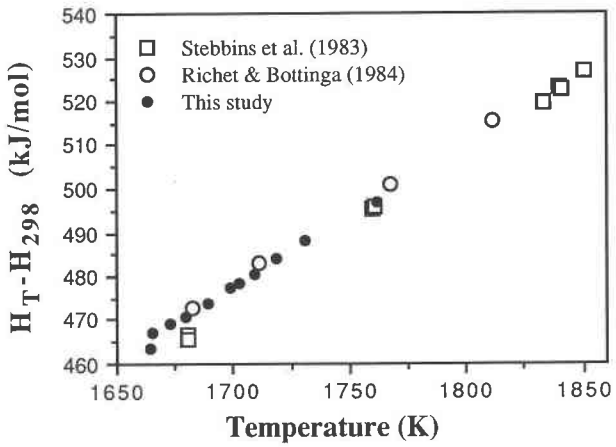

Fig. 5. Enthalpy (referenced to crystalline diopside) vs. temperature in the stable liquid region only. The measured liquid heat contents from this study are compared to those reported by Richet and Bottinga (1984) and Stebbins et al. (1983). The derived heat capacity of liquid diopside using all three data sets is 334 ± 7 J/mol·K.

Integration of the observed heat capacity between 1606 and 1665 K leads to a total enthalpy change of 157.2 kJ/mol. However, integration of the extrapolated heat capacity of crystalline diopside within this interval contributes 19.5 kJ/mol to the total enthalpy. The enthalpy due to fusion alone is thus the difference between these values, namely 137.7 kJ/mol, and is in close agreement with the values obtained by Stebbins et al. (1983), Richet and Bottinga (1984), and Ziegler and Navrotsky (1986). It is, however, about 10 kJ/mol higher than the value of 128 kJ/mol obtained by Ferrier (1968). The error in the value presented in this study stems primarily from uncertainties in the heat capacity data during incongruent melting. An uncertainty in C_P of ±40 J/mol·K throughout the melting interval of 59 K leads to an estimated uncertainty in the enthalpy of fusion of ±2.4 kJ/mol.

We conclude that the Setaram HT1500 calorimeter in step-scan mode can provide values of heat content and heat of fusion comparable in accuracy and precision to those obtained by conventional methods. The individual heat capacities obtained show significant scatter (5% for crystal and 12% for melt), but this scatter appears random enough that the integral quantities (H_T-H_{298}) and average heat capacities are well constrained.

Observations on incongruent melting and a preliminary crystallization study by scanning calorimetry

The abrupt rise in the heat capacity of crystalline diopside 59 K below the melting point reported previously is suggestive of incongruent melting. However, the possibility of the presence of a second phase, such as tiny dendritic crystals of either wollastonite or forsterite, must first be examined. According to the phase diagram for Mg_2SiO_4-$CaMgSi_2O_6$ of both Bowen (1914) and Kushiro

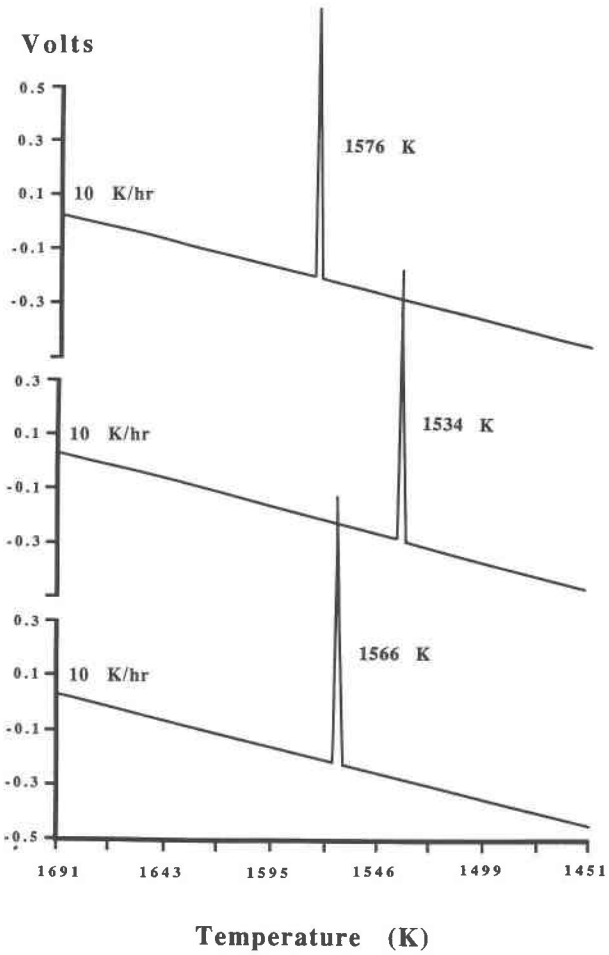

Fig. 6. Three crystallization experiments in the calorimeter at a constant cooling rate of 10 K/h. In each experiment, the initial temperature was 1691 K. Despite identical conditions, a single large heat effect as a result of the crystallization of clinopyroxene and wollastonite was observed at three temperatures: 1576, 1534, and 1566 K.

and Schairer (1963), the lowest solidus temperature occurs at approximately 1654 K at a bulk composition of Fo_6Di_{94}. Similarly, the phase diagram for $MgSiO_3$-$CaSiO_3$ of Schairer and Bowen (1942) indicates that the lowest solidus temperature occurs at approximately 1631 K if any wollastonite crystals (up to 38 wt%) coexist with diopside. Thus, neither the presence of 6 mol% forsterite crystals (above the detection limit of the XRD) nor small amounts of wollastonite crystals (potentially below our detection limits) can explain the depression of the diopside solidus by 59 K.

Further support for the incongruent melting of diopside is found in the initial report of Biggar and O'Hara (1969), which was later confirmed by Kushiro (1973) in a detailed electron microprobe study. Biggar and O'Hara (1969) observed, in the melting of pure crystalline diopside, a small amount of glass in charges quenched from as low as 1623 K (suggesting an incongruency of at least 42 K). From our determinations of enthalpy throughout the melting interval of diopside (Fig. 4 and Table 2), we estimate that about 5% melting occurs at 1623 K. Melt percentages smaller than this are probably difficult to detect by optical methods or by drop calorimetry.

The electron microprobe study of Kushiro (1973) on crystalline diopside samples equilibrated and quenched from temperatures as low as 17 K below the melting point reported previously provides information on the evolving composition of both the liquid and crystalline phases. The initial melt is enriched in $CaSiO_3$ and SiO_2 components relative to pure $CaMgSi_2O_6$. Correspondingly, the residual diopside solid solution is increasingly enriched in the forsterite and enstatite components as melting progresses. Kushiro (1973) noted further that one sample in his study, which did not quench rapidly from 1655 K, contained a small amount of fine-grained, irregular crystals between large crystals of diopside solid solution. The glass in this product had the composition of CaO = 40.7 wt%, MgO = 3.80 wt%, and SiO_2 = 54.9 wt%; this composition lies well within the liquidus field of pseudowollastonite and is far from the expected glass composition. These results, taken in conjunction with the kinetic crystallization experiments of Kirkpatrick et al. (1981), suggest that the fine-grained quench crystals may have been forsterite.

Kirkpatrick et al. (1981) performed crystallization experiments on diopside liquid over a range of cooling rates from 10 K/h to 300 K/h. In all cases, metastable crystallization of forsterite was observed prior to the combined crystallization of a clinopyroxene solid solution and wollastonite. At the slowest cooling rate of 10 K/h, the temperature interval over which forsterite crystallized alone was 39 K, beginning at 1508 K. Clinopyroxene and wollastonite were not found in the quenched charges until 1469 K, where no coexisting glass was found, indicating extremely rapid growth rates.

One of the objectives of our study was to repeat the crystallization experiments of Kirkpatrick et al. (1981) in the calorimeter. Specifically, we wanted to see if we could identify the heat effect due to the crystallization of forsterite prior to that of clinopyroxene and wollastonite. An initial crystallization experiment in the calorimeter at a constant cooling rate of 30 K/h from 1715 K resulted in a single, large heat effect at 1545 K (see Fig. 6). This crystalline sample was examined by electron microprobe analysis, and only two phases were observed, a Mg-rich diopside solid solution and a Mg-bearing wollastonite phase. A second crystallization experiment was conducted in the calorimeter at a slower cooling rate of 10 K/h, beginning at 1691 K; again a single, large heat effect was observed, although this time at 1576 K (see Fig. 6). This latter experiment was repeated twice more at the same cooling rate and from the same initial temperature of 1691 K, and each time only a single, large heat effect was seen. However, the temperature at which crystallization was observed was variable; in the second experiment, rapid crystallization was at 1534 K, whereas in the third

experiment it took place at 1566 K (see Fig. 6). This variability illustrates the difficulty in quantifying nucleation rates in silicate melts.

Two aspects of our crystallization experiments differ from those of Kirkpatrick et al. (1981). The first is that we observe crystallization 89–131 K below the liquidus of 1665 K at a constant cooling rate of 10 K/h, whereas Kirkpatrick et al. (1981) observed crystallization of clinopyroxene and wollastonite 196 K below 1665 K. Our observation of crystallization 65–107 K earlier than found by Kirkpatrick et al. (1981) may reflect the fact that our samples were held in capsules and not on Pt loops; thus, a greater surface area for heterogeneous nucleation was available. The second difference is that we did not observe a heat effect that could be correlated to the crystallization of forsterite prior to clinopyroxene and wollastonite. However, forsterite may have crystallized in our charges, but in such small quantities that it could not be detected. We estimate the minimum amount of forsterite that is required to crystallize before the heat effect can be resolved in our calorimetry. We assume that the minimum heat effect detectable in continuous scanning experiments is approximately 1% of the crystallization peak observed for clinopyroxene and wollastonite. The combined heat of fusion of these two phases will be less than that of pure diopside at 1665 K (137.7 kJ/mol) because of the lower heat of fusion of wollastonite relative to diopside (Adamkovicova et al., 1980). The combined heat of fusion of clinopyroxene and wollastonite between 1534 and 1576 K is approximately 100–120 kJ/mol. Therefore, to resolve a heat effect that is within 1% of this value, enough forsterite must crystallize to produce a heat effect of at least 1–1.2 kJ/mol. The minimum amount of crystallization necessary for detection in the scanning experiments can be calculated by extrapolating the heat of fusion of forsterite from its melting point (2163 K) to 1508 K, the initial temperature at which Kirkpatrick et al. (1981) observed forsterite. The heat of fusion at 2163 K is approximately 114 kJ/mol (Navrotsky et al., 1989) and was extrapolated to 1508 K using the heat capacity for crystalline forsterite of Robie et al. (1979) and the heat capacity for liquid Mg_2SiO_4 calculated from the algorithm of Stebbins et al. (1984); this led to a value of 62 kJ/mol. Therefore, to produce a heat effect on the order of 1–1.2 kJ/mol, about 1.6 mol% of forsterite must crystallize at 1508 K. However, Kirkpatrick et al. (1981) observed forsterite crystallizing over an interval of 39 K, unlike the rapid and complete crystallization of clinopyroxene and wollastonite within a few degrees. As a consequence, if approximately 1.6 mol% forsterite crystallized continuously every 5 K throughout the crystallization interval (39 K), then a total of 12 mol% of forsterite could crystallize in the capsule without detection by scanning calorimetry. Thus, the absence of a heat effect that can be attributed to forsterite does not preclude its presence in quantities comparable to those observed by Kirkpatrick et al. (1981).

This type of calculation can be extended to the drop calorimetric experiments of Ferrier (1968) and the anomalous low heat of fusion (128 kJ/mol) reported in that study. The presence of a clinopyroxene and a wollastonite phase in our samples cooled at a rate of 30 K/h suggests that the enthalpy of fusion reported by Ferrier (1968) for diopside may in fact represent a combined heat of fusion of two phases. Ferrier's (1968) drop calorimetric enthalpy measurements on liquid diopside differ from both those of Stebbins et al. (1983) and those of Richet and Bottinga (1984), in that the diopside sample dropped into the calorimetric block crystallized and did not form a glass. The experiments of Kushiro (1973) and Kirkpatrick et al. (1981) indicate that a wollastonite phase could easily have crystallized along with diopside solid solution during the drop experiments of Ferrier (1968). The much lower value of the heat of fusion reported by Ferrier (1968) may, therefore, be the result of the smaller heat of fusion of the wollastonite phase relative to diopside. This depression in the heat of fusion observed by Ferrier (1968) can be used to estimate the amount of wollastonite that may have crystallized in his drop experiments. The enthalpy of fusion of pure wollastonite at its melting point (1821 K) was measured by Adamkovicova et al. (1980; 57.3 kJ/mol) and can be extrapolated using the heat capacity for crystalline wollastonite in Robie et al. (1979) and the heat capacity for liquid $CaSiO_3$ calculated from the algorithm of Stebbins et al. (1984). The heat of fusion of wollastonite at 1665 K thus estimated is 50.6 kJ/mol. Combining this value with the heat of fusion for pure diopside obtained in this study (137.7 kJ/mol) indicates that approximately 11 mol% of wollastonite may have formed in Ferrier's experiments.

Conclusions

Scanning calorimetric measurements applied to compounds that melt incongruently provide detailed information on the behavior of heat capacity throughout a melting interval. This sensitivity to melting is a unique feature of the step-scan method that is not accessible by conventional drop calorimetric techniques. As a consequence, high temperature scanning calorimetry is particularly well suited for direct measurements of melting and crystallization in magmatic systems, where primary interest lies in the distribution of enthalpy over a liquidus-solidus interval.

For systems that melt congruently, stepping up and down through the melting-freezing point can provide data on the heat of fusion directly and rapidly. Even for samples that melt over an interval of temperature, data can be obtained less tediously than by repeated transposed-temperature drops. The data obtained are generally more precise, as well, since samples are not dropped but are tamped tightly into sample crucibles, improving thermal conduction between the sample and the thermopiles of the calorimeter.

Perhaps the most interesting aspect of the scanning method is that it can be applied to direct studies of the kinetics of crystallization. This is particularly relevant to

natural liquids, as both the order and composition of crystallizing phases depend critically upon the cooling rate (Walker et al., 1976; Grove and Raudsepp, 1978). Thus, quantifying latent heats of fusion during crystallization will allow the effect of a variable cooling rate on the evolving heat content of a magma to be evaluated.

Acknowledgments

This work was supported by the National Science Foundation (grant EAR-8803215). We thank Katharine Cashman and Susan Swapp for their assistance with the JEOL 8600 microprobe.

References cited

Adamkovicova, K., Kosa, L., and Proks, I. (1980) The heat of fusion of $CaSiO_3$. Silikaty, 24, 193–201.

Berman, R.G., and Brown, T.H. (1984) A thermodynamic model for multicomponent melts, with application to the system CaO-Al_2O_3-SiO_2. Geochimica et Cosmochimica Acta, 45, 661–678.

——— (1985) Heat capacity of minerals in the system Na_2O-K_2O-CaO-MgO-FeO-Fe_2O_3-Al_2O_3-SiO_2-TiO_2-H_2O-CO_2: Representation, estimation and high temperature extrapolation. Contributions to Mineralogy and Petrology, 89, 168–183.

——— (1987) Development of models for multicomponent melts: Analysis of synthetic systems. In Mineralogical Society of America, Reviews in Mineralogy, 17, 405–442.

Biggar, G.M., and O'Hara, M.J. (1969) Solid solutions at atmospheric pressure in the system CaO-MgO-SiO_2 with special reference to the instabilities of diopside, akermanite and monticellite. Progress in Experimental Petrology, First Report, 86–96.

Bowen, N.L. (1914) The ternary system diopside-forsterite-silica. American Journal of Science, 33, 551–573.

Brandeis, G., and Jaupart, C. (1984) Nucleation, crystal growth and the thermal regime of cooling magmas. Journal of Geophysical Research, 89, 10161–10177.

Castanet, R., and Bergman, C. (1977) Thermodynamic functions and structure of gallium + tellurium liquid alloys. Journal of Chemical Thermodynamics, 9, 1127–1132.

Ferrier, A. (1968) Mesure de l'enthalpie du diopside synthétique entre 298 et 1885 K. Comptes Rendues Academie des Science de Paris, C, 267, 101–103.

Gaune-Escard, M., and Bros, J.-P. (1974) High temperature calorimetry up to 1800 K. Canadian Metallurgy Quarterly, 13, 335–338.

Ghiorso, M. (1987) Modeling magmatic systems: Thermodynamic relations. In Mineralogical Society of America Reviews in Mineralogy, 17, 443–465.

——— (1991) Temperatures in and around cooling magma bodies. In L.L. Perchuk, Ed., Progress in metamorphic and magmatic petrology, p. 387–410. Cambridge Press, Cambridge, England.

Ghiorso, M., and Carmichael, I.S.E. (1985) Chemical mass transfer in magmatic processes. II. Applications in equilibrium crystallization, fractionation and assimilation. Contributions to Mineralogy and Petrology, 90, 121–141.

Ghiorso, M., Carmichael, I.S.E., Rivers, M.L., and Sack, R.O. (1983) The Gibbs free energy of mixing of natural silicate liquids; an expanded regular solution approximation for the calculation of magmatic intensive variables. Contributions to Mineralogy and Petrology, 84, 107–145.

Grove, T.L., and Raudsepp, M. (1978) Effects of kinetics on the crystallization of quartz normative basalt 15587: An experimental study. Proceedings of the Eighth Lunar Science Conference, 1501–1520.

Kirkpatrick, R.J., Kuo, L.C., and Melchoir, J. (1981) Crystal growth in incongruently-melting compositions: Programmed cooling experiments with diopside. American Mineralogist, 66, 223–241.

Kushiro, I. (1973) Incongruent melting of pure diopside. Carnegie Institution of Washington Year Book, 72, 708–710.

Kushiro, I., and Schairer, J.F. (1963) New data on the system diopside-forsterite-silica. Carnegie Institution of Washington Year Book, 62, 95–103.

Lange, R.A., and Carmichael, I.S.E. (1987) Densities of K_2O-Na_2O-CaO-MgO-FeO-Fe_2O_3-Al_2O_3-TiO_2-SiO_2 liquids: New measurements and derived partial molar properties. Geochimica et Cosmochimica Acta, 51, 2931–2946.

Navrotsky, A., Ziegler, D., Oestrike, R., and Manier, P. (1989) Calorimetry of silicate melts at 1773 K: Measurements of enthalpies of fusion and of mixing in the systems diopside-anorthite-albite and anorthite-forsterite. Contributions to Mineralogy and Petrology, 101, 122–130.

Pool, M.S., Bredel, B., and Schultheiss, E. (1979) Application of the Setaram high temperature calorimeter for determination of mixing enthalpies of liquid alloys. Thermochimica Acta, 28, 349–358.

Richet, P., and Bottinga, Y. (1984) Anorthite, andesine, wollastonite, diopside, cordierite and pyrope: Thermodynamics of melting, glass transitions, and properties of the amorphous phases. Earth and Planetary Science Letters, 67, 415–432.

Robie, R.A., Hemingway, B.S., and Fisher, J.R. (1979) Thermodynamic properties of minerals and related substances at 298.15 K and 1 bar (10^5 Pascals) pressure and at higher temperature. U.S. Geological Survey Bulletin 1452, revised edition.

Schairer, J.F., and Bowen, N.L. (1942) The binary system $CaSiO_3$-diopside and the relations between $CaSiO_3$ and akermanite. American Journal of Science, 240, 725–742.

Stebbins, J.F., Carmichael, I.S.E., and Weill, D.E. (1983) The high temperature liquid and glass heat contents and the heats of fusion of diopside, albite, sanidine and nepheline. American Mineralogist, 68, 717–730.

Stebbins, J.F., Carmichael, I.S.E., and Moret, L.K. (1984) Heat capacities and entropies of silicate liquids and glasses. Contributions to Mineralogy and Petrology, 86, 131–148.

Wagner, H. (1932) Zur Thermochemie der Metasilikate des Kalziums und Magnesiums und des Diopsids. Zeitschrift für Anorganische und Allgemeine Chemie, 208, 1–20.

Walker, D., Kirkpatrick, R.J., Longhi, J., and Hays, J.F. (1976) Crystallization history of lunar picrite basalt sample 12002: Phase equilibrium and cooling rate studies. Bulletin of the Geological Society, 87, 646–656.

White, W.P. (1919) Silicate specific heats. American Journal of Science 47, 1–44.

Ziegler, D., and Navrotsky, A. (1986) Direct measurement of the enthalpy of fusion of diopside. Geochimica et Cosmochimica Acta, 50, 2461–2466.

Manuscript received March 5, 1990
Manuscript accepted February 26, 1991